

Effect of titanium on microstructure and fluidity of Al–B₄C composites

Z. Zhang · K. Fortin · A. Charette ·
X.-G. Chen

Received: 15 July 2010 / Accepted: 17 December 2010 / Published online: 7 January 2011
© Springer Science+Business Media, LLC 2011

Abstract The effect of Ti on the interfacial reactions, microstructural characteristics, and the related fluidity of Al–12%B₄C composites has been investigated. Without Ti addition, B₄C decomposed heavily during holding, and a large quantity of reaction-induced compounds, Al₃BC and AlB₂, was generated. When Ti was added, a TiB₂ layer was built surrounding B₄C particle surfaces, which acted as a diffusion barrier to separate B₄C from liquid aluminum. Thus, the decomposition of B₄C slowed down remarkably. The fluidity of the composite without Ti was the shortest of all composites and deteriorated quickly during the holding time. The fluidity of the composite melt was improved significantly with increased Ti levels. The optimum Ti level for the best fluidity results lied between 1.0 and 1.5%. The solid particle volume and the particle agglomeration are the two main factors influencing the fluidity.

Introduction

Al–B₄C metal matrix composites (MMCs) are targeted as new advanced materials for nuclear industry primarily due to their ability to capture neutrons as well as their low density, high thermal conductivity, and stiffness [1–3]. It is well known that the interface region between the matrix and ceramic particles has a great deal of importance in determining the ultimate properties of the composite materials [4, 5]. It was observed that B₄C was unstable in liquid aluminum [6, 7]. To understand the interface reactions between aluminum and B₄C, an investigation using

powder metallurgy with a ratio of Al, B, and C of 40:48:12 at.% was carried out [8]. The samples were heated for 160 h at different temperatures. It was demonstrated that the interface reaction products were Al₃BC and AlB₂ at temperatures ranging from 677 to 827 °C. In the liquid mixing process, the contact time of B₄C particles with molten aluminum is quite long, usually ranging from tens of minutes to several hours. The decomposition of B₄C was severe and the reaction products were observed as AlB₂, Al–C and Al–B–C compounds [6, 9]. Literature related to the interface reactions of Al–B₄C composites by the liquid mixing process is scarce.

In recent years, substantial progresses in the development of castable Al–B₄C MMCs with the liquid mixing process have been made [1, 2, 6, 10]. Ti was introduced into Al–B₄C composites in order to limit the decomposition of B₄C particles and enhances their wettability in liquid aluminum [3, 6, 11]. It was reported that, by adding Ti, a Ti-rich layer surrounding B₄C particle surfaces was formed. Using a transmission electron microscope, it was confirmed that the Ti-rich layer consisted mainly of TiB₂ particles in examples of Al–7%Si–10%B₄C and Al–10%B₄C composites [12, 13]. This layer limited the interfacial reactions and improved the fluidity of Al–B₄C composites [6].

The fluidity can be defined as the ability of molten metal to flow in a long channel of small cross section, and the length the metal flows before it is stopped by solidification is the measure of fluidity [14]. Good fluidity is a basic requirement for the composites to be produced in the casting processes [15]. The fluidity of Al-based metal matrix composites has been studied by several researchers [16–19]. The volume fraction of solid particles significantly influences the fluidity of Al-based composites. The more solid particles in the composites, the shorter flow

Z. Zhang (✉) · K. Fortin · A. Charette · X.-G. Chen
Université du Québec à Chicoutimi, Chicoutimi,
QC G7H 2B1, Canada
e-mail: zhan_zhang@uqac.ca

length the composites has [17]. Moreover, the size and shape of reinforcing particles, particle agglomeration, presence of oxide films, and reaction induced particles might impact the composite fluidity [17–21]. In the Al–B₄C composites, however, the relationship between microstructure and fluidity in the Al–B₄C composites with different Ti concentrations is not yet fully understood.

The aim of this study is to clarify the effect of Ti on the microstructural characteristics, the variation of particle volume fraction attributed to interfacial reactions, and the related fluidity of Al–B₄C composites in the liquid mixing process.

Experimental

For the preparation of the experimental composites, prefabricated Rio Tinton Alcan AA1100-18 vol.% B₄C without and with 0.75 wt% Ti cast billets was used in this investigation. The average size of the B₄C particles (F400) was approximately 17 μm. During the batch operation, commercially pure aluminum was first melt in an electrical resistance furnace. The prefabricated cast billets with 0.75 wt% Ti and an Al-10 wt% Ti master alloy were then added into the molten aluminum in the desired proportions in order to obtain the final composites consisting of 12 vol.% B₄C containing 0.5, 0.75, 1.0, 1.5, 2.0, and 3.0 wt% Ti, respectively. For the non-Ti containing composite, the prefabricated cast billets without Ti were directly diluted in liquid pure aluminum to obtain an Al–12% B₄C composite.

The processing time of the remelting, from adding the prefabricated cast billets into liquid aluminum to reaching 750 °C, is about 30 min. A vacuum fluidity test set-up was used for the evaluation of the fluidity. In the fluidity tests, the composite melt was held at 750 ± 2 °C for 2 h under mechanical stirring, thus ensuring a uniform distribution of B₄C particles in the liquid. The pressure supplied by a vacuum system in the set-up was kept at 215 mm Hg while the composite melt filled a 6 mm inside diameter glass

tube. After solidification of the composite in the glass tube, the length of the composite in the tube (length of flow) was measured for the fluidity evaluation. A fluidity sample was regularly taken at every 10–15 min. The details of the test set-up and the sampling position for metallographic examination are given in Fig. 1.

An image analyzer (CLEMEX JS-2000, PE4.0) equipped with a 3-CCD color video camera (SONY DXC-950P) was used for quantitative microstructure characterization such as particle volume fraction measurement. Under an optical microcopy, all solid particles have different colors and gray scale. For examples, B₄C particles show a dark color while the interfacial reaction-induced phases, Al₃BC and AlB₂ particles, have a gray and a yellow color, respectively. The volume fraction of these solid particles was measured by the image analyzer at a 500× magnification based on the particle colors and gray scale [22].

A scanning electron microscope (SEM, JSM-6480LV) equipped with an energy dispersive spectrometer (EDS) and a transmission electron microscope (TEM, JEM 2100F) were used to identify and measure the interfacial reaction products in the composites.

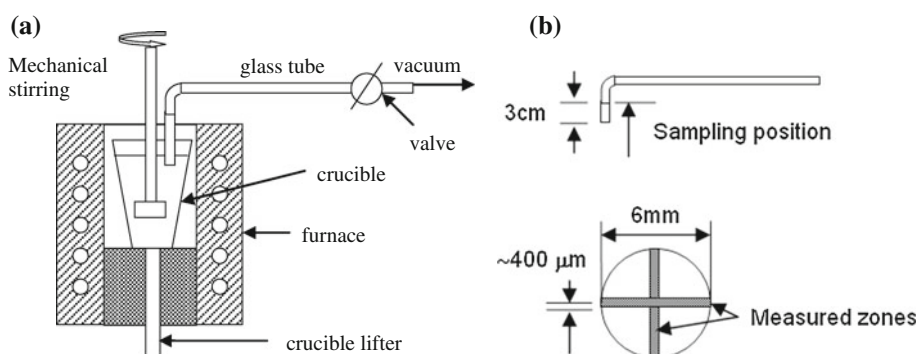
Results and discussion

Microstructure of Al–12% B₄C composites without Ti

Thermodynamic calculation

Figure 2a shows the isothermal section of the Al–B–C phase diagram at 750 °C, calculated using the ThermoCalc software and a database supplied by L. Kaufman (private communications, 2008). The results agree well with the previous research [8]. In this isothermal section, the following compounds appeared: Al₈B₄C₇, Al₄C₃, Al₃BC, Al₃B₄₈C₂, AlB₂, AlB₁₂, and B₄C. At the Al-rich corner, there were two three-phase triangles: Al_(l)–AlB_{2(s)}–Al₃BC_(s) triangle, and Al_(l)–Al₄C_{3(s)}–Al₃BC_(s) triangle. The dashed line between Al and B₄C is drawn on the diagram to

Fig. 1 **a** Set-up sketch of a vacuum fluidity test, **b** sampling position, and quantitative analysis zones on a cross section of a sample



represent the Al–B₄C composites (B:C = 4:1) in the Al–B–C system. It is evident that up to 52 at.% (32 vol.%) of B₄C, all Al–B₄C composites were located in the Al_(l)–AlB_{2(s)}–Al₃BC_(s) triangle. Following the dashed line toward B₄C, above 52 and 60 at.% B₄C, AlB₁₂ and another complex boron carbide Al₃B₄₈C₂ may occur. It is worth noting that B₄C did not show in the Al_(l)–AlB_{2(s)}–Al₃BC_(s) triangle. This indicated that B₄C particles were thermodynamically unstable in liquid aluminum and would continue to decompose as long as they contact liquid aluminum. Thus, the reaction between liquid aluminum and B₄C takes place at the interfaces Al/B₄C according to

$$9\text{Al} + 2\text{B}_4\text{C} = 2\text{Al}_3\text{BC} + 3\text{AlB}_2 \quad (1)$$

Two reaction induced compounds, Al₃BC and AlB₂, were produced.

The isopleths phase diagram of Al–B₄C is shown in Fig. 2b, calculated based on Kaufman's database (private communication, 2008). The compounds appearing in this isopleths diagram are the same as those occurring in 750 °C isothermal section phase diagram (Fig. 2a). When

the B₄C fraction was less than 52 at.% (32 vol.%), Al₃BC and AlB₂ were stable from the room temperature to 1000 °C according to the phase diagram. As the temperature was higher than 1000 °C, AlB₁₂ and later Al₄C₃ would appear. Above 52 at.% of B₄C, other compounds Al₈B₄C₇, Al₃B₄₈C₂, and AlB₁₂ could occur, which made the phase diagram more complex.

Microstructure of the composite without Ti

The optical microstructures of the Al–12% B₄C composite samples with 5 and 120 min holding times are shown in Fig. 3 and represent the microstructure of the samples with a short and a long holding time, respectively. Shortly after remelting (5 min sample), two interfacial reaction induced phases appeared in the composite microstructure (Fig. 3a). One phase was yellow color with blocky-like forms, and another one around B₄C particles was gray color with a smaller size under optical microscopic observation. Using SEM and TEM, it was identified that the yellow phase was AlB₂ and the gray phase was Al₃BC. This microstructural

Fig. 2 Calculated phase diagrams: **a** Al–B–C isothermal section at 750 °C, **b** Al–B₄C isopleths phase diagram

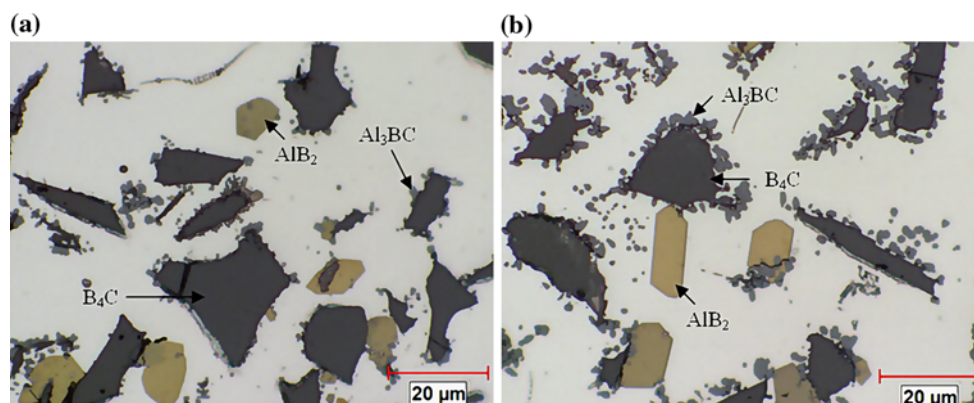
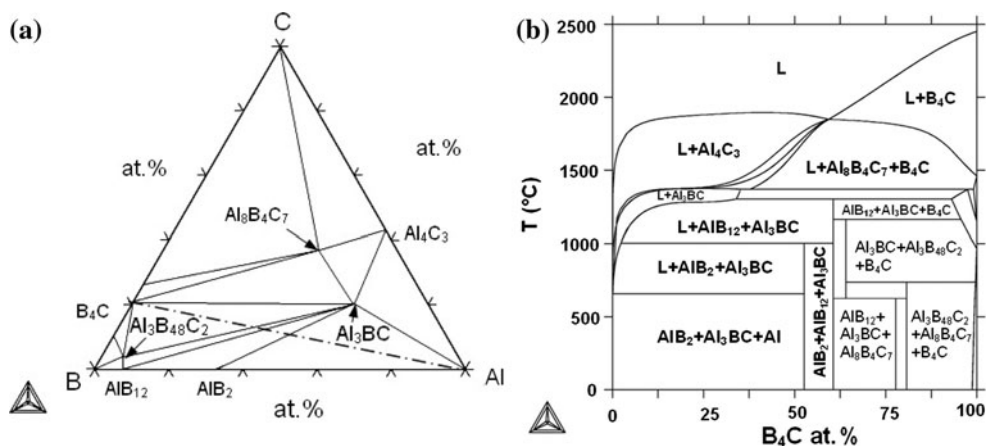


Fig. 3 Optical microstructure of Al–12%B₄C at 750°C, **a** 5 min holding, **b** 120 min holding

observation was consistent with the calculated phase diagram (Fig. 2). When prolonging the holding time (Fig. 3b), the amount and the size of the two compounds, AlB_2 and Al_3BC , increased remarkably.

Figure 4 shows the SEM micrographs of different holding times and reveals more details of the interfacial reaction around B_4C particles. As B_4C particles gradually decomposed (Fig. 4a), Al_3BC crystals precipitated and grew on the B_4C surfaces. The interfacial reaction took place between liquid aluminum and free B_4C surfaces, which was a typical liquid diffusion controlled process. With prolonged reaction time (Fig. 4b), a severe attack on B_4C by liquid aluminum was obvious and B_4C surfaces became rough and irregular. Al_3BC grew from the B_4C surface toward the matrix and their size became larger. Some of the Al_3BC detached from the B_4C particles probably because of the liquid convection. Although Al_3BC crystals occupied more B_4C surfaces with a longer holding time, they did not spread around the B_4C surfaces as their main growth direction was toward the liquid. There were always some free B_4C surfaces or free channels between Al_3BC crystals toward the liquid (Fig. 4b). On the other hand, the reaction product, AlB_2 , precipitated when the liquid supersaturated with boron and most of them grew in the matrix instead of on the B_4C surfaces. It is evident that, as the reaction continued, the interfacial reaction (1) was always dominated by the liquid diffusion. As a result, the decomposition of B_4C occurred at a high rate and a large quantity of reaction compounds (Al_3BC and AlB_2) was produced.

Microstructure of Al– B_4C composites with different Ti levels

Interfacial structure

To understand the effect of Ti on the microstructure of Al– B_4C composites, the microstructure of Al–12% B_4C

composites containing different Ti levels was examined by means of optical and electron microscopes. The backscattered electron images of SEM revealed that there was a Ti-rich layer covering the B_4C particle surface in the Ti contained Al– B_4C composites (Fig. 5). This was found in other studies as well [6, 10–12]. At a low Ti level (0.5%), this layer was quite thin and did not cover all the B_4C surfaces (Fig. 5a). With an increased reaction time, the B_4C particles continued to decompose remarkably and the reaction products Al_3BC occurred inside and outside of the Ti-rich layer (Fig. 5b). At a high Ti level (1.5%), the Ti-rich layer was thick and completely enclosed B_4C surfaces (Fig. 5c). After a long holding period, the decomposition of B_4C particles was less obvious (Fig. 5d).

A close observation using TEM showed the microstructure of the interfacial region in great detail (Fig. 6). Al_3BC and TiB_2 were identified in the interface Al/ B_4C by means of electron diffraction in selected areas. It was seen that the B_4C surface first covers a tiny Al_3BC layer and then followed the Ti-rich layer that was composed of TiB_2 crystals. This Ti-rich layer enclosed the Al_3BC layer and the B_4C surface, and acted as a diffusion barrier. It was obvious that, in this case, liquid aluminum could no longer directly contact B_4C particles. The interfacial reaction in the Ti contained Al– B_4C composites became the solid diffusion controlled process.

The Ti-rich layer was divided into two sub-layers (Fig. 6). On a nanometer scale, the inside sub-layer consisted of a great number of fine TiB_2 crystals and continuously enclosed the Al_3BC layer and the B_4C surface. This sub-layer acted as a real diffusion barrier in the separation of B_4C from liquid aluminum. The outside sub-layer was composed of coarse plate-like TiB_2 particles (particle size: 0.2–1 μm). These coarse TiB_2 particles randomly grew from the fine TiB_2 crystals toward the Al-matrix. Owing to its discontinuous and less dense nature, this sub-layer did not enclose all interfacial surfaces and played a less effective role as a diffusion barrier.

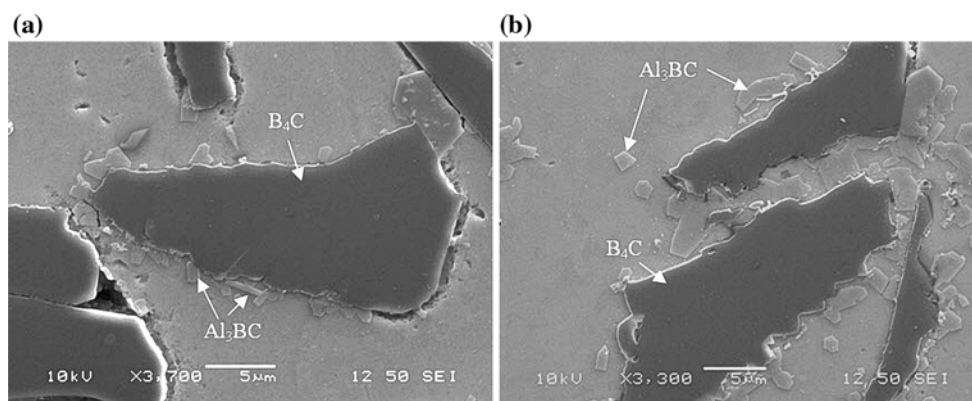


Fig. 4 SEM second electron images of Al–12% B_4C at 750°C. **a** 5 min holding, **b** 120 min holding

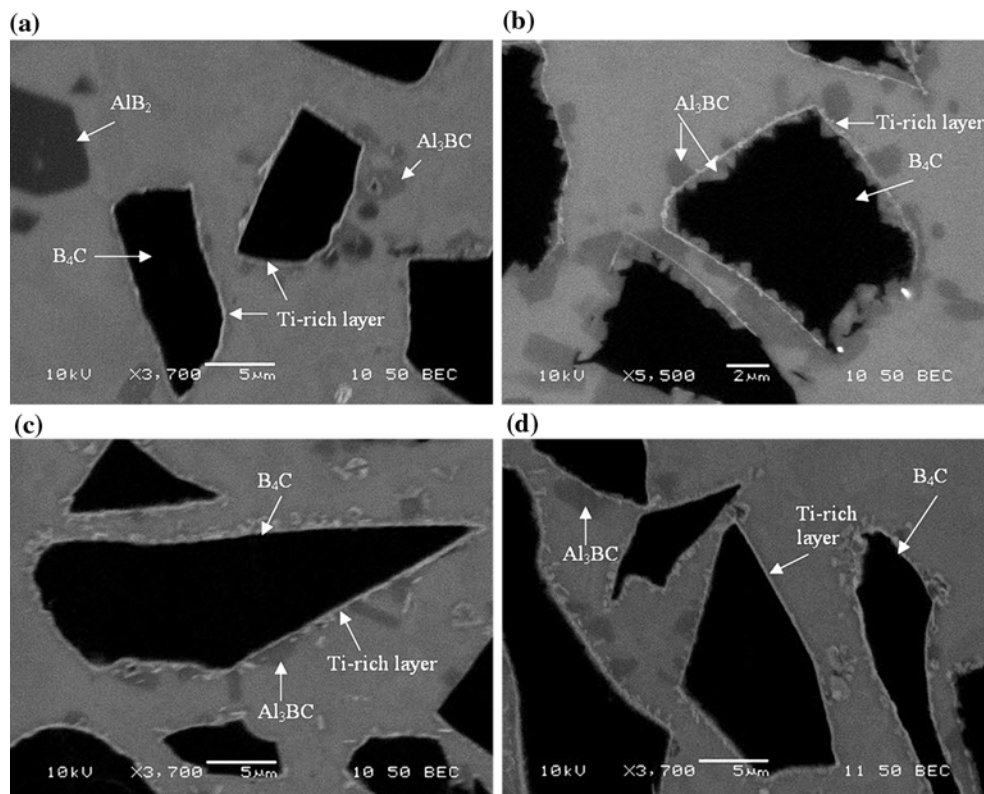


Fig. 5 Backscattered electron images of the microstructure of Al–12%B₄C composites containing 0.5%Ti with **a** 5 min holding and **b** 120 min holding, and 1.5%Ti with **c** 2 min holding and **d** 120 min holding

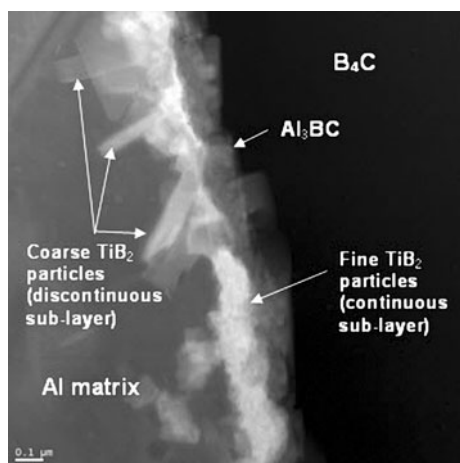


Fig. 6 STEM dark field micrograph of the 1.0%Ti composite, showing the TiB₂ layers in the interface region in great details

In general, the thickness of the Ti-rich layer was less than 1 μm. Although its thickness was not very uniform in the micro scale, the average thickness of the Ti-layer in Al–B₄C composites was a function of the Ti levels. The results of the average thickness measurement are given in Table 1 and show that the more Ti in the composite, the thicker the Ti-rich layer is.

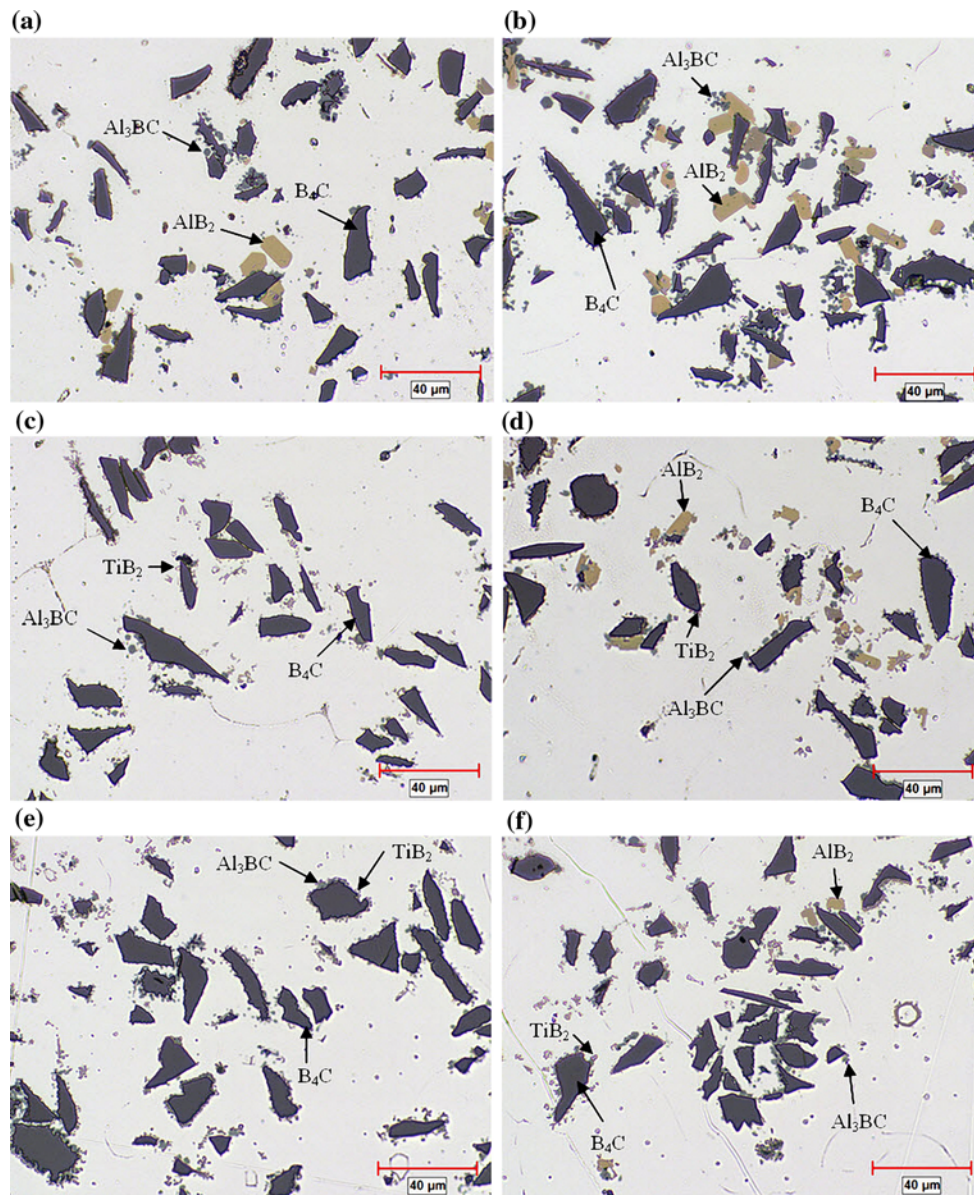
Microstructure of the composites with Ti

The optical microstructure of the Al–12%B₄C composite samples with typical Ti levels are shown in Figs. 7 and 8. For each Ti level, two micrographs are displayed, which represent the microstructure with initial holding and after a long holding period, respectively. It should be mentioned that it takes approximately 30 min from adding prefabricated Al–B₄C billets into liquid aluminum to reaching 750 °C (beginning of the holding period). During that time, the interfacial reaction has already occurred.

In the low level Ti (0.5%), major reaction phases Al₃BC and AlB₂ coexist alongside B₄C particles at the initial holding period (Fig. 7a). As the holding period was prolonged, the amount of these two phases increased quickly, indicating a severe interfacial reaction. The decomposition of B₄C was therefore ongoing. After 2 h of holding, a number of Al₃BC and AlB₂ particles were generated around the B₄C particles (Fig. 7b). The size and distribution of both phases were different. Having a small size, the Al₃BC particles were mostly connected to or surrounded the B₄C particles. The AlB₂ showed individual particles in the blocky form and were often not directly attached to B₄C particles. As the Ti level increased, the major reaction products shifted to Al₃BC and TiB₂ (Fig. 7c,e). When Ti

Table 1 Thickness of Ti-rich layer on B_4C particles (5 min holding; standard deviation in parenthesis)

%Ti in the composites	Continuous sub-layer (fine TiB_2 crystals) Average thickness (nm)	Discontinuous sub-layer (coarse plate-like TiB_2) Average thickness (nm)	Number of the measured locations
0.5	83 (19)	145 (28)	12
1.5	121 (22)	207 (37)	12
3.0	160 (36)	213 (45)	12

**Fig. 7** Optical microstructure of Al-12%B₄C composites containing: 0.5%Ti composite with **a** 5 min holding, **b** 120 min holding; 1.0%Ti composite with **c** 5 min holding, **d** 150 min holding; 1.5%Ti composite with **e** 5 min holding, **f** 120 min holding

reached 1.5%, only Al_3BC and TiB_2 particles were found around the B_4C particles, and AlB_2 disappeared. After 2 h of holding, both reaction phases (Al_3BC and TiB_2)

increased slightly and few AlB_2 particles scattered in the microstructure (Fig. 7d, f). The more Ti contained, the less AlB_2 particles appeared in the composites. It is evident that

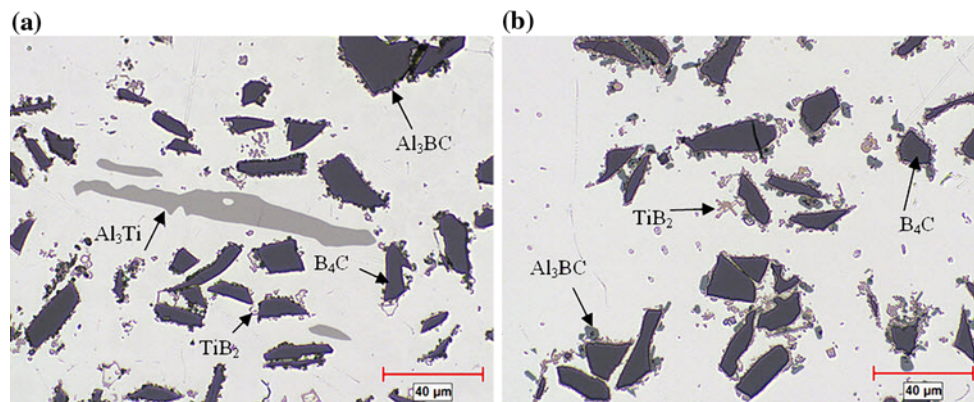


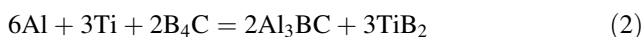
Fig. 8 Microstructure of 3.0%Ti composite: optical image of the sample with **a** 5 min holding, **b** 120 min holding

the interfacial reaction and therefore the decomposition of B_4C slow down significantly with an increase of Ti. With further Ti level increases (toward 3%), large plate-like Al_3Ti intermetallic particles, besides Al_3BC and TiB_2 appeared in the matrix at the early stage of holding (Fig. 8a), which indicated an excess of Ti in the Al-matrix. During further holding, these Al_3Ti intermetallic particles gradually decomposed and converted into many small TiB_2 particles that dispersed in the Al-matrix (Fig. 8b).

Discussion of the influence of Ti on B_4C stability and microstructure

Results of thermodynamic calculation and experiments clearly show that B_4C particles were unstable in liquid aluminum. When B_4C contacted liquid aluminum, B_4C particles reacted instantly with aluminum, and the reaction compounds Al_3BC and AlB_2 were generated. However, both the Al_3BC and AlB_2 compounds were unable to enclose the B_4C surfaces. The interfacial reaction (1) was controlled by the liquid diffusion and showed the fastest rate of B_4C decomposition.

With Ti addition in the Al– B_4C system, the following interfacial reaction (2) became more favorable than the interfacial reaction (1) due to the fact that Ti had a much higher affinity with boron than aluminum, and the Gibbs energies of the formation of TiB_2 (–331.0 kJ/mol) was more negative than that of AlB_2 (–108.8 kJ/mol) at 750 °C (Kaufman, private communication, 2008):



The reaction product TiB_2 built a Ti-rich layer surrounding the B_4C surfaces and the decomposition of B_4C slowed down remarkably.

In the low Ti level (0.5% in Al–12% B_4C), the Ti-rich layer was thin and more or less discontinuous. The B_4C decomposition was controlled by a fast solid diffusion through the loose structure layer, and it was therefore slower than that of the composite without Ti. With appropriate Ti

levels (1.0–1.5% in Al–12% B_4C), the TiB_2 layer became dense and continued enclosing all B_4C surfaces. The B_4C was completely separated from the liquid aluminum. The interfacial reactions were dominated by the slow solid diffusion. Any further decomposition of B_4C was restricted by a dense structure layer. When an excess of Ti was added into the composite (2–3% in Al–12% B_4C), Al_3Ti intermetallics came out in the Al-matrix. This indicated that the aluminum matrix and B_4C could no longer absorb the rest of the Ti in the composite melt. As the holding period was prolonged, the Al_3Ti intermetallics gradually decomposed and combined with boron atoms to form TiB_2 .

Influence of Ti on the fluidity of Al– B_4C composites

Fluidity evolution

Figure 9 shows the fluidity evolution of the Al–12 vol.% B_4C composites with different Ti levels. The flow length of the composite without Ti was the shortest of all composites, and it rapidly deteriorated during the holding time. After only 1 h, the fluidity reached the lowest plateau, at which point the molten composite was almost unable to flow. The fluidity of the composite containing 0.5%Ti was improved, but the tendency of the fluidity deterioration was similar to the composite without Ti. By increasing the Ti levels from 0.5 to 1.5%Ti, the fluidity of composites augmented significantly. Simultaneously, the fluidity deterioration slowed down considerably during the holding. As the Ti levels further increased toward 2 and 3%, the fluidity of the composite was no longer improved but rather decreased by some degrees. Results of the fluidity indicated that the optimum Ti levels for this composite lied between 1.0 and 1.5%.

Fraction of reaction products and total solid particles

The volume fractions of the reaction products and total solid particles in all composites were quantitatively measured by

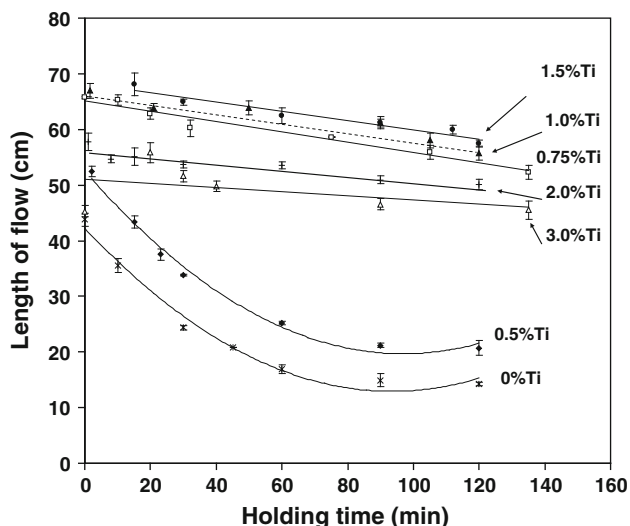


Fig. 9 Fluidity evolution of the composite melt with and without titanium

the optical image analyzer. Results of the volume fraction of the reaction products including Al_3BC , AlB_2 , TiB_2 , and Al_3Ti , as a function of the holding time, are given in Fig. 10a. At the beginning of the holding, the reaction products for all composites ranged between 6 and 7%. The volume fraction of reaction products generally increased when prolonging the holding time. However, the reaction products in the composite without Ti augmented very rapidly. Within a 2-h holding period, the amount of the reaction products almost doubled and reached 13%. In the low Ti level (0.5%), the rate of the fraction increase already slowed down. As the Ti increased to 1.5%, the reaction products remained at the lowest level. During the 2-h holding period, their amount only increased from 6.5% (initial) to 7.5%. However, when the Ti went beyond 1.5%Ti, the fraction of the reaction products rose again, due to the appearance of Al_3Ti and excessive TiB_2 in the matrix.

The volume fractions of the total solid particles in all composites are shown in Fig. 10b. Here, the total particles include all the solid particles: B_4C , Al_3BC , AlB_2 , TiB_2 , and Al_3Ti . The tendency was similar to that of the fraction of reaction products. This is due to the fact that the variation of the total particle amount was mainly contributed by the changes of the reaction products in the composites. Moreover, the cooling of the composite melt from liquid to solid in the thin glass tube is very fast (only few seconds), i.e., the amount of any precipitates during solidification should be very small. Therefore, it is reasonable to believe that the change of the particle volume fraction is taken place during liquid holding period.

It had been reported that the fluidity decreases with the increase of the volume fraction of solid particles in Al-based composites [15, 16]. The composite without Ti generated the highest amount of the reaction products and hence the maximum amount of the total solid particles. Therefore, it had the lowest fluidity during the holding period. When increasing the Ti levels, the volume fractions of the reaction products and the total solid particles were limited, and therefore, the fluidity was greatly improved. The composite containing 1.0–1.5%Ti had the minimum solid particle fraction and led to the best fluidity results.

It should be mentioned that the total particle fraction of the 0.5%Ti composite during holding was very close to that of the 3.0%Ti composite. However, the flow length of the former after 2 h holding (18 mm) was much shorter than that of the latter (45 mm). It was found that, besides the particle fraction, the particle agglomeration could also affect the fluidity of Al-based composites. This will be discussed later.

Particle agglomeration and effective volume fraction

In the composite materials, large agglomerates were often visible, and they appeared in two forms [13]: dense particles

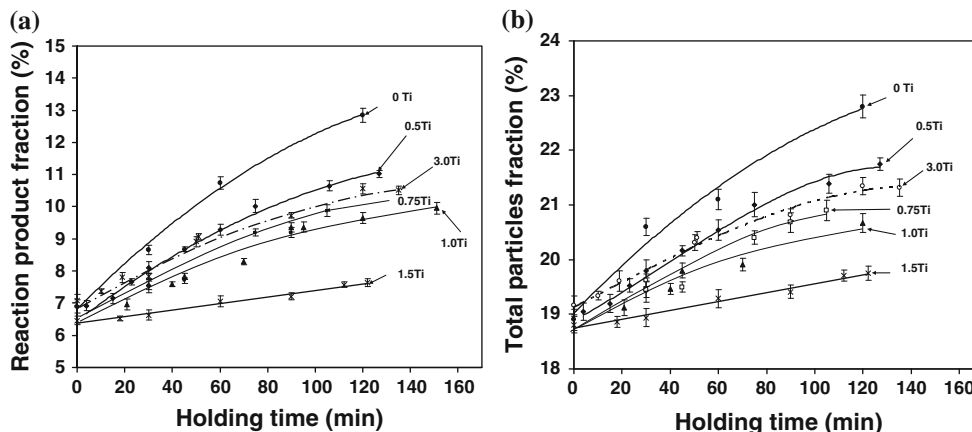


Fig. 10 a Volume fraction of reaction products. b total solid particle volume fraction in the composites

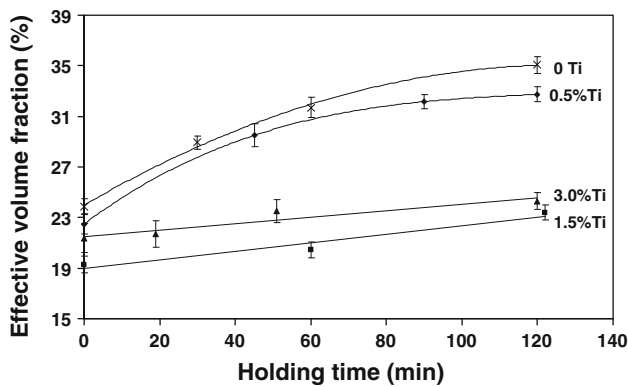


Fig. 11 Effective volume fraction of solid particles at some typical Ti levels

clusters and particle networks. Forming during the melting process, these agglomerates moved as a whole mass and occupied a much greater space in fluid flowing. Therefore, they had higher flow resistance than the sum of the individual solid particles they contained. To combine both impacts of the particle agglomerates and individual particles, the effective volume fraction of solid particles was introduced. This is defined as the enclosed area of whole particle agglomerates and the volume of the remaining solid particles that do not belong to these agglomerates. The effective volume fractions of solid particles in the composites with typical Ti levels are shown in Fig. 11.

At the beginning of the holding period, the composite without Ti already had the highest effective particle volume fraction. Since the total particle volumes of all composites (without and with Ti) were almost similar at the beginning of the holding time (Fig. 10b), this indicated that the composite without Ti had the highest particle agglomerates at the beginning. When increasing the Ti level, the particle agglomerates decreased. Compatibly, the sample without Ti had the shortest flow length and the fluidity of the composites was improved when increasing the Ti level. As the holding time increased, the effective particle volume fractions in the composites without Ti and with low Ti (0.5%) increased more rapidly than that with the Ti contained composites. After a 2-h holding period, the effective particle volume fractions reached 35% in the composite without Ti while it was only 23% for the 1.5%Ti composite. Taking into account the particle agglomeration, the effective volume fraction of the particles corresponded better with the fluidity results than the volume fraction of the total solid particles.

Conclusions

1. In the Al–12%B₄C composite without Ti, B₄C decomposed heavily and generated a large quantity of

reaction products Al₃BC and AlB₂. The observation is consistent with the thermodynamic calculation of the Al–B–C phase diagram.

2. Ti addition in Al–B₄C composites formed a TiB₂ layer enclosing the B₄C surface and acted as a diffusion barrier to separate B₄C from liquid aluminum. With appropriate Ti levels, B₄C was completely separated from liquid aluminum. The decomposition of B₄C and hence the quantity of the reaction products remained at a low level during a long holding period.
3. The fluidity of the composite without Ti was the shortest of all the composites and deteriorated quickly during the holding time. The fluidity of the composite melt was improved significantly when increasing the Ti level. The optimum Ti level for the best fluidity result lied between 1.0 and 1.5% for the Al–12% B₄C composite.
4. The solid particle volume and the particle agglomeration were the two main factors influencing the fluidity of the composite melt. The effective volume fraction of particles was introduced to take into account both factors during the fluid flow. The fluidity evolution of the composites with different Ti levels during holding was well consistent with the changes of the effective volume fraction of particles.

Acknowledgements The authors would like to acknowledge the financial support of the Natural Sciences and Engineering Research Council of Canada (NSERC), Rio Tinto Alcan and the Centre Québécois de Recherche et de Développement de l'Aluminium (CQRDA).

References

1. Chen X-G (2006) In: Gupta N, Hunt WH (eds) Proceedings of TMS (2006), symposium on Solidification process of metal matrix composites, San Antonio, March 2006, p 343
2. Chen X-G, Hark R (2008) In: Yin W, Das SK (eds) Proceedings of TMS (2008), Symposium on Aluminum alloys: fabrication, characterization and applications, New Orleans, p 3
3. Kennedy AR (2002) *J Mater Sci* 37:317. doi:10.1023/A:1013600328599
4. Lloyd DJ (1997) In: Mallick PK (ed) Composites engineering handbook. Marcel Dekker, Inc, New York, p 631
5. Chawla KK (2005) In: Cahn RW, Haasen P, Kramer EJ (eds) Materials science and technology, vol 13/14. Wiley-VCH, Weinheim, p 137
6. Chen X-G (2005) In: Schlesinger ME (eds) EPD Congress 2005, TMS 2005, San Francisco, p 101
7. Lloyd DJ, Lagacé HP, Mcleod AD (1990) In: Ishida H (ed) Controlled interphases in composite materials. Elsevier Science Publishing Co. Inc, New York, p 362
8. Viala JC, Bouix J, Gonzalez G, Esnouf C (1997) *J Mater Sci* 32:4559. doi:10.1023/A:1018625402103
9. Shorowordi KM, Laoui T, Haseeb ASMA, Celis JP, Froyen L (2003) *J Mater Proc Technol* 142:738
10. Fortin JY, Sheehy J, Jean C, Brisson P, Harnisch U, Doutre D, Chen X-G (2009) US Patent US 7,572,692 B2, 21 July 2009

11. Kennedy AR, Brampton B (2001) *Scripta Mater* 44:1077
12. Zhang Z, Chen X-G, Charette A (2007) *J Mater Sci* 42:7354. doi:[10.1007/s10853-007-1554-5](https://doi.org/10.1007/s10853-007-1554-5)
13. Zhang Z, Chen X-G, Charette A (2009) *J Mater Sci* 44:492. doi:[10.1007/s10853-008-3097-9](https://doi.org/10.1007/s10853-008-3097-9)
14. Flemings MC (1974) *Solidification processing*. McGraw-Hill Book Company, New York, p 219
15. Campbell J (1999) *Casting*. Butterworth Heinemann, Oxford, p 75
16. Yarandi FM, Rohatgi PK, Ray S (1993) *J Mater Eng Perform* 2(3):359
17. Rohatgi P, Asthana R (2001) *JOM* 53(9):9
18. Surappa MK, Rohatgi PK (1981) *Metall Mater Trans B* 12B:327
19. Kolsgaard A, Brusethaug S (1994) *Mater Sci Technol* 10:545
20. Ravi VA, Frydrych DJ, Nagelberg AS (1994) *AFS Trans* 102:891
21. Ravi KR, Pillai RM, Pai BC, Chakraborty M (2007) *Metall Mater Trans A* 38:2531
22. Gokhale AM (2004) In: Voort G (ed) *ASM handbook*, vol 9. The Materials Information Company, Materials Park, p 428